Physics Letters B ••• (••••) ••••••

Contents lists available at ScienceDirect

Physics Letters B

www.elsevier.com/locate/physletb

The continuum spectrum of hypernuclear trios

M. Schäfer [a,b], B. Bazak [c], N. Barnea [c], J. Mareš [b]

[a] Czech Technical University in Prague, Faculty of Nuclear Sciences and Physical Engineering, Břehová 7, 11519 Prague 1, Czech Republic
[b] Nuclear Physics Institute of the Czech Academy of Sciences, 25069 Řež, Czech Republic
[c] The Racah Institute of Physics, The Hebrew University, Jerusalem 9190401, Israel

ARTICLE INFO

Article history:
Received 19 March 2020
Received in revised form 5 July 2020
Accepted 8 July 2020
Available online xxxx
Editor: W. Haxton

Keywords:
Hypernuclei
Effective field theory
Hypertriton
Λnn
Resonance

ABSTRACT

The spectrum of hypernuclear trios composed of a Λ baryon and two nucleons is the subject of an ongoing experimental campaign, aiming to study the interaction of the Λ particle with a neutron, and the 3-body Λ-nucleon-nucleon force. In this manuscript we utilize baryonic effective field theory at leading order, constrained to reproduce the available low energy light hypernuclear data, to study the continuum spectrum of such hypernuclear trios. Using the complex scaling method and the inverse analytic continuation in the coupling constant method we find the existence of a virtual state in the Λnp $J^\pi = 3/2^+$ channel, leading to cross-section enhancement near threshold. For the Λnn $J^\pi = 1/2^+$ channel we predict a resonance state. Depending, however, on the value of the ΛN scattering length, the resonance pole moves from the physical to the unphysical complex energy sheet within the experimental bounds.

1. Introduction

Understanding the interaction between nucleons and a Λ hyperon is the subject of an ongoing experimental and theoretical campaign [1]. In the last few years much effort is dedicated to the study of hypernuclear trios (ΛNN) aiming to determine the unknown Λ-neutron (Λn) interaction, and the ΛNN 3-body force. The latter is known to have a crucial effect in the nuclear equation of state at high density, and therefore on our understanding of neutron stars.

The Λ-nucleon interaction is not strong enough to bind a ΛN pair, making the hypertriton ${}^3_\Lambda\mathrm{H}(I=0,\ J^\pi=1/2^+)$ the lightest hypernuclei. It is weakly bound with a Λ separation energy $B_\Lambda = 0.13 \pm 0.05$ MeV [2]. The experimental search for other bound hypernuclear trios has found no evidence for the hypertriton state ${}^3_\Lambda\mathrm{H}^*$, ${}^3_\Lambda\mathrm{H}(I=0,\ J^\pi=3/2^+)$, indicating that the singlet $s=0$ ΛN interaction is somewhat stronger than the triplet $s=1$ interaction.

Recently, the HypHI collaboration [3] has claimed evidence for a bound Λnn state, ${}^3_\Lambda n(I=1,\ J^\pi=1/2^+)$. However, this observation contradicts theoretical analyses demonstrating that such a bound state cannot exist. Since the first calculation by Dalitz and Downs [4], numerous theoretical studies of $I=0,1$ and $J=1/2,3/2$ ΛNN states have been performed, confirming the observation that no bound Λnn and ${}^3_\Lambda\mathrm{H}(I=0,\ J^\pi=3/2^+)$ exist within Faddeev calculations for separable potentials [5,6], chiral constituent quark model of YN interactions [7,8] or the Nijmegen hyperon-nucleon potentials [9]. The same conclusion was drawn in [10] within variational calculations using YN model, simulating the realistic Nijmegen interaction. The Λnn system was also studied within a baryonic (pionless) effective field theory ($\not\pi$EFT) [11,12], however, due to uncertainty in fixing the three-body Λnn force no firm predictions of its stability could be made.

In spite of the theoretical consensus regarding a bound Λnn, the nature of hypernuclear ΛNN trios remains a subject of an ongoing discussion [13]. Specifically, the search for the Λnn system is a goal of the JLab E12-17-003 experiment [14], and the study of the ${}^3_\Lambda\mathrm{H}(I=0,\ J^\pi=3/2^+)$ state is part of the JLab proposal P12-19-002 [15].

Regardless the apparent interest, the possible existence of Λnn and ${}^3_\Lambda\mathrm{H}^*$ hypernuclear continuum states has been directly addressed in only few theoretical works. Calculating zeros of the three-body Jost function, Belyaev et al. found a very wide, near-threshold, Λnn resonance [16]. Afnan and Gibson [17] using Faddeev calculation and separable potentials, fitted to reproduce ΛN and NN scattering length and effective range, concluded that the Λnn state exists as a sub-threshold resonance. They also found that a small increase of the ΛN interaction strength shifts the resonance position above threshold and thus yields an observable resonance. We are not aware of any direct calculation of the ${}^3_\Lambda\mathrm{H}^*$ continuum state, however, as Garcilazo et al. concluded, there is a

E-mail addresses: m.schafer@ujf.cas.cz (M. Schäfer), betzalel.bazak@mail.huji.ac.il (B. Bazak), nir@phys.huji.ac.il (N. Barnea), mares@ujf.cas.cz (J. Mareš).

https://doi.org/10.1016/j.physletb.2020.135614

hint of near-threshold pole which gives rise to large Λd scattering length in $J^\pi = 3/2^+$ channel [7].

The aforementioned continuum studies [7,8,16,17] were limited to $A = 3$ systems. Therefore, the predictive power of their interaction models was not verified against the available experimental B_Λ data in e.g. 4-body or 5-body s-shell hypernuclei. In fact, applying a gaussian potential mimicking the low energy behavior of the separable potential of [17] we find substantial overbinding in these systems. Given the relatively poorly known ΛN scattering parameters, and the precise B_Λ data, such comprehensive study is called for.

Motivated by the debate regarding the nature of the hypernuclear 3-body states, and the soon to be published JLab E12-17-003 Λnn results [14], in the present work we report on precise few-body calculations of the hypernuclear ΛNN bound and continuum spectrum, using Hamiltonians constructed at leading order (LO) in $\not\pi$EFT [18]. This $\not\pi$EFT is an extension, including Λ hyperons, of the n, p nuclear $\not\pi$EFT Hamiltonian, first reported in [19,20] and more recently used to study lattice-nuclei in [21–24]. At LO $\not\pi$EFT contains both 2-body and 3-body contact interactions. The theory's parameters, i.e. the 2- and 3-body low-energy constants (LECs), were fitted to reproduce the $\Lambda N, NN$ scattering lengths, ^{3}H binding energy, and the available 3,4-body B_Λ data [18]. The predictive power of the theory was tested against the measured $^5_\Lambda$He separation energy [18,49]. The $\not\pi$EFT breakup scale can be associated with 2-pion exchange $2m_\pi$, or the threshold value for exciting ΣN pair. These two values are remarkably close. Assuming a typical energy scale E_Λ of about 1 MeV, the momentum scale $Q \approx \sqrt{2M_\Lambda E_\Lambda} = 47$ MeV/c, suggesting a $\not\pi$EFT expansion parameter $(Q/2m_\pi) \approx 0.2$. This implies a $\not\pi$EFT LO accuracy of order $(Q/2m_\pi)^2 \approx 4\%$.

The 3-body calculations were performed with the Stochastic Variational Method (SVM) expanding the wave function on a correlated gaussian basis [25,26], the continuum states were located using the Complex Scaling Method (CSM) [34], or the Inverse Analytic Continuation in the Coupling Constant (IACCC) Method [48].

Our main findings are: (a) The possible existence of a bound Λnn, or $^3_\Lambda$H* state is ruled out, confirming findings of previous theoretical studies [4–10,16,17]. (b) The excited state of hypertriton, $^3_\Lambda$H$^*(J^\pi = 3/2^+)$, is a virtual state. (c) The Λnn state is a resonance pole near the three-body threshold in a complex energy plane. The position of this pole depends on the value of the ΛN scattering length. Within the current bounds on the ΛN scattering length it can either be a real resonance or a sub-threshold resonance.

2. Calculational details

2.1. Hypernuclear $\not\pi$EFT at LO

At LO the $\not\pi$EFT of neutrons, protons and Λ-hyperons is given by the Lagrangian density

$$\mathcal{L} = N^\dagger\Big(i\partial_0 + \frac{\nabla^2}{2M_N}\Big)N + \Lambda^\dagger\Big(i\partial_0 + \frac{\nabla^2}{2M_\Lambda}\Big)\Lambda + \mathcal{L}_{2B} + \mathcal{L}_{3B} \qquad (1)$$

where N and Λ are nucleon and Λ-hyperon fields, respectively, and $\mathcal{L}_{2B}, \mathcal{L}_{3B}$ are 2-body, and 3-body, s-wave contact interactions, with no derivatives. These contact interactions are regularized by introducing a local gaussian regulator with momentum cutoff λ, see e.g. [27],

$$\delta_\lambda(\mathbf{r}) = \left(\frac{\lambda}{2\sqrt{\pi}}\right)^3 \exp\left(-\frac{\lambda^2}{4}\mathbf{r}^2\right) \qquad (2)$$

that smears the Dirac delta appearing in the contact terms over distances $\sim \lambda^{-1}$. This procedure yields Hamiltonian containing two-body V_2 and three-body V_3 interactions

Table 1
Input spin-singlet $a_0^{\Lambda N}$ and spin-triplet $a_1^{\Lambda N}$ scattering lengths (in fm), used to fit the hypernuclear 2-body LECs. Also shown is the spin-independent combination of ΛN scattering lengths $\bar{a}^{\Lambda N} = (3a_1^{\Lambda N} + a_0^{\Lambda N})/4$.

model	Reference	$a_0^{\Lambda N}$	$a_1^{\Lambda N}$	$\bar{a}^{\Lambda N}$
Alexander B	[28]	-1.80	-1.60	-1.65
NSC97f	[29]	-2.60	-1.71	-1.93
χEFT(LO)	[30]	-1.91	-1.23	-1.40
χEFT(NLO)	[31]	-2.91	-1.54	-1.88

$$V_2 = \sum_{I,S} C_\lambda^{I,S} \sum_{i<j} \mathcal{P}_{ij}^{I,S} \delta_\lambda(r_{ij})$$
$$V_3 = \sum_{I,S} D_\lambda^{I,S} \sum_{i<j<k} \mathcal{Q}_{ijk}^{I,S} \sum_{cyc} \delta_\lambda(r_{ij})\delta_\lambda(r_{jk}), \qquad (3)$$

where $\mathcal{P}_{ij}^{I,S}$ and $\mathcal{Q}_{ijk}^{I,S}$ are the 2- and 3-body projection operators into an s-wave isospin-spin (I, S) channels. The cutoff λ dependent parameters $C_\lambda^{I,S}$, and $D_\lambda^{I,S}$ are the 2- and 3-body LECs, fixed for each λ by the appropriate renormalization condition. For λ higher than the breakup scale of the theory ($\lambda > 2m_\pi$), observables posses residual cutoff dependence, at LO $O(Q/\lambda)$, suppressed with λ approaching the renormalization group invariant limit $\lambda \to \infty$ [18].

In total there are 4 two-body (NN, ΛN), and 4 three-body (NNN, ΛNN) LECs. The nuclear LECs $C_\lambda^{I=0,S=1}$, $C_\lambda^{I=1,S=0}$, and $D_\lambda^{I=1/2,S=1/2}$ are fitted to the deuteron binding energy, NN spin-singlet scattering length a_0^{NN}, and to the triton binding energy, respectively. The hypernuclear two-body LECs $C_\lambda^{I=1/2,S=0}$ and $C_\lambda^{I=1/2,S=1}$ are fixed by the ΛN < spin-singlet $a_0^{\Lambda N}$ and spin-triplet $a_1^{\Lambda N}$ scattering lengths. The three-body hypernuclear LECs $D_\lambda^{I=0,S=1/2}$, $D_\lambda^{I=1,S=1/2}$, and $D_\lambda^{I=0,S=3/2}$ are fitted to the experimental Λ separation energies $B_\Lambda(^3_\Lambda\text{H})$, $B_\Lambda(^4_\Lambda\text{H})$, and the excitation energy $E_{\rm exc}(^4_\Lambda\text{H}^*)$.

Since $a_0^{\Lambda N}$ and $a_1^{\Lambda N}$ are not well constrained by experiment, we consider different values both as given by direct analysis of experimental data [28], or as predicted by several ΛN interaction models [29–31], see Table 1. For the particular values of the LECs see [18].

2.2. The stochastic variational method

The A-body Schrödinger equation is solved expanding the wave function Ψ in correlated gaussians basis [25]

$$\Psi = \sum_i c_i\, \psi_i = \sum_i c_i\, \hat{\mathcal{A}}\left\{\exp\left(-\frac{1}{2}\mathbf{x}^T A_i \mathbf{x}\right)\chi_{SM_S}^i \xi_{IM_I}^i\right\}, \qquad (4)$$

where $\hat{\mathcal{A}}$ stands for the antisymmetrization operator over nucleons, $\mathbf{x} = (\mathbf{x}_1, ..., \mathbf{x}_{A-1})$ denotes a set of Jacobi vectors, and $\chi_{SM_S}^i$ ($\xi_{IM_I}^i$) is the spin (isospin) part. The information about interparticle correlations is contained in the $(A-1)$ dimensional positive-definite symmetric matrix A_i. Once we fix all basis functions ψ_i, both energies and coefficients c_i are obtained through diagonalization of the Hamiltonian matrix. The $A(A-1)/2$ nonlinear variational parameters contained in each A_i matrix are determined using the Stochastic Variational Method (SVM) [25,26].

Unlike bound states, continuum wave functions are not square-integrable. Therefore, resonances or virtual states can not be directly described using an L^2 basis set of correlated gaussians. Techniques such as CSM or IACCC have to be used to study such states with a correlated gaussians. Below we discuss in some detail the techniques we applied in our study.

2.3. The complex scaling method

The CSM [34] is a reliable tool to study few-body resonances [35]. The basic idea in the CSM is to locate resonances introducing complex rotation of coordinates and momenta

$$U(\theta)\mathbf{r} = \mathbf{r}e^{\mathrm{i}\theta}, \quad U(\theta)\mathbf{k} = \mathbf{k}e^{-\mathrm{i}\theta}, \tag{5}$$

that transforms the continuum states into integrable L^2 states. This transformation rotate continuum state energies by 2θ uncovering a section of the second energy plane between the real axis and a ray defined by $|\arg E| = 2\theta$, exposing resonances with argument $\theta_r = \arctan(\Gamma/2E_r)/2$ smaller than θ. Here, $E_r = \mathrm{Re}(E)$ is the resonance energy and $\Gamma = -2\mathrm{Im}(E)$ is the width. Using gaussian regulator (3) the rotation angle is restricted to be $\theta < \frac{\pi}{4}$, to prevent divergence of the rotated gaussian, limiting the scope of the CSM.

The SVM method uses the variational principle as a tool to optimize the nonlinear basis parameters A_i (4), minimizing the basis size. This does not apply to resonance states, making it a highly non trivial problem to choose the appropriate basis. Here, we present a new efficient procedure to determine the basis set for an accurate description of resonance states. To optimize the basis, we supplement the Hamiltonian H with an additional harmonic oscillator (HO) trap

$$H^{\mathrm{trap}}(b) = H + V^{\mathrm{HO}}(b), \quad V^{\mathrm{HO}}(b) = \frac{\hbar^2}{2mb^4}\sum_{j<k} r_{jk}^2, \tag{6}$$

where m is an arbitrary mass scale, and b is the HO trap length. The potential $V^{\mathrm{HO}}(b)$ gives rise to a HO spectrum of the ground and excited states which is affected by the presence of a resonance in the Hamiltonian H [42]. For a given trap length b we select basis states ψ_i (4) using the SVM, optimizing the variational parameters for the ground state energy and then subsequently for excited states energies up to $E_{\max} > E_r + \Gamma/2$. The SVM procedure prefers basis states which promote interparticle distances r_{jk} in a specific region given by the trap length b. Increasing b we enlarge the typical radius of the correlated gaussians ψ_i. For large enough b, the CSM resonance solution for the Hamiltonian H starts to stabilize and both the short range and the suppressed long range asymptotic parts of a resonance wave function are described sufficiently well. In order to further enhance the accuracy of our CSM solution, we use a grid $\{b_k\}$, of a HO trap lengths, and for each grid point we independently select correlated gaussians basis. Then we merge basis states determined for each b_k into a larger basis while ensuring linear independence and numerical stability of the overlap matrix. We have found that this procedure works well for both narrow, and broad resonances.

2.4. Inverse analytic continuation in the coupling constant method

The Analytic Continuation in the Coupling Constant (ACCC) method [43] has been successfully applied in various calculations of few-body resonances and virtual states [44,45]. Moreover, it was pointed out that the ACCC method provides rather convenient way how to extend applicability of the SVM into the continuum region [44,46]. We consider a few-body Hamiltonian consisting of the physical part H and an auxiliary attractive potential V^{aux}

$$H^{\mathrm{IACCC}} = H + \alpha\, V^{\mathrm{aux}}, \tag{7}$$

which introduces a bound state for a certain value of α, but ensures that the physical dissociation thresholds for the various subsystems remain unaffected. By decreasing the strength α the bound state moves closer to the threshold and for a certain α_0 it turns into a resonance or virtual state. It has been demonstrated for a two-body system that in the vicinity of the branching point α_0 the square root of an energy $k = \sqrt{E}$ behaves as $k \approx (\alpha - \alpha_0)$ for s-wave ($l = 0$) and $k \approx \sqrt{\alpha - \alpha_0}$ for $l > 0$ [43]. Defining new variable $x = \sqrt{\alpha - \alpha_0}$ one obtains two branches $k(x)$ and $k(-x)$ where the former one describes motion of the S-matrix pole assigned to a bound state on a positive imaginary k-axis to the third quadrant of a k-plane. Using analyticity of the function $k(x)$ one can continue from a bound region $\alpha > \alpha_0$ to a resonance region $\alpha < \alpha_0$. In practice this is done by constructing a Padé approximant

$$k(x) \approx \mathrm{i}\frac{\sum_{j=0}^{M} c_j x^j}{1 + \sum_{j=1}^{N} d_j x^j} \tag{8}$$

for the function $k(x)$ using $M + N + 1$ bound state solutions $\{(x_j, k_j); j = 1, \ldots, M + N + 1\}$ for different values of $\alpha > \alpha_0$. The evaluation of the Padé approximant (8) at $x = \sqrt{-\alpha_0}$ yields complex k which is assigned to the physical resonance solution $k^2 = E_r - \mathrm{i}\Gamma/2$ corresponding to the Hamiltonian H. For more details regarding the ACCC method see [47].

The ACCC method suffers from two drawbacks which are predominantly of numerical nature. The first issue is high sensitivity of the numerical solution to precise determination of the branching point value α_0 [43]. The second obstacle appears with increasing orders M and N of the Padé approximant (8) when the numerical solution starts to deteriorate.

Rather recently Horáček et al. [48] have introduced a modified version of the ACCC method called the Inverse Analytic Continuation in the Coupling Constant (IACCC) method which provides more robust numerical stability. Starting in the same manner as in the ACCC case, we consider the Hamiltonian (7) and calculate series of bound states for different values of $\alpha > \alpha_0$. Next, we construct a Padé approximant of a function $\alpha(\kappa)$, where $\kappa = -\mathrm{i}k$, using a relevant set of bound state solutions

$$\alpha(\kappa) \approx \frac{P_M(\kappa)}{Q_N(\kappa)} = \frac{\sum_{j=0}^{M} c_j \kappa^j}{1 + \sum_{j=1}^{N} d_j \kappa^j}. \tag{9}$$

The parameters of the physical resonance or virtual state pole are then readily obtained by setting $\alpha = 0$ as the physical root of a simple polynomial equation $P_M(\kappa) = 0$.

To ensure that the properties of the 2-body part of the Hamiltonian, such as scattering lengths or deuteron binding energy, remain unaffected, we choose the auxiliary potential to be an attractive 3-body force. The natural choice is to select it to have the same form as the $\not\pi$EFT 3-body potential (3),

$$V_3^{\mathrm{IACCC}} = d_\lambda^{I,S} \sum_{i<j<k} Q_{ijk}^{I,S} \sum_{\mathrm{cyc}} e^{-\frac{\lambda^2}{4}\left(r_{ij}^2 + r_{jk}^2\right)}, \tag{10}$$

where the amplitude $d_\lambda^{I,S}$ defines its strength, corresponding to the parameter α in Eq. (7), and is negative for an attractive auxiliary potential.

The accuracy of our IACCC resonance solutions in the fourth quadrant of the complex energy plane, $\mathrm{Re}(E) > 0$, $\mathrm{Im}(E) < 0$, are better than $\approx 10^{-3}$ MeV. These results compare very well with the CSM calculations in their region of applicability $\theta < \pi/4$.

3. Results

Using $\not\pi$EFT at LO with the LECs fitted to the available data as described earlier [18], we find no bound Λnn or ${}^{3}_{\Lambda}\mathrm{H}^*$ states. Further examining the hypothetical existence of these states, we found that they are incompatible with the well measured $A = 4, 5$ hypernuclear spectrum.

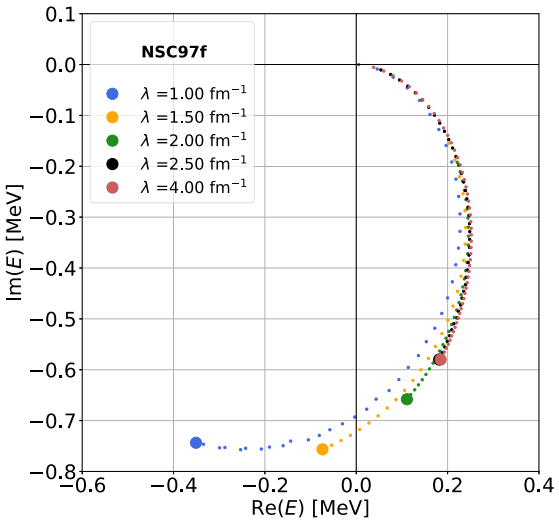

Fig. 1. Trajectories of the Λnn resonance pole in the complex energy plane determined by a decreasing attractive strength of the auxiliary three-body force $d_\lambda^{I=1,S=1/2}$ for several cutoffs λ and the NSC97f set of ΛN scattering lengths. Small dots mark IACCC solutions for different $d_\lambda^{I=1,S=1/2}$, larger symbols stand for the physical position of the Λnn pole ($d_\lambda^{I=1,S=1/2}=0$). Notice the almost overlapping trajectories for $\lambda=2.50$ fm^{-1} and $\lambda=4.00$ fm^{-1}.

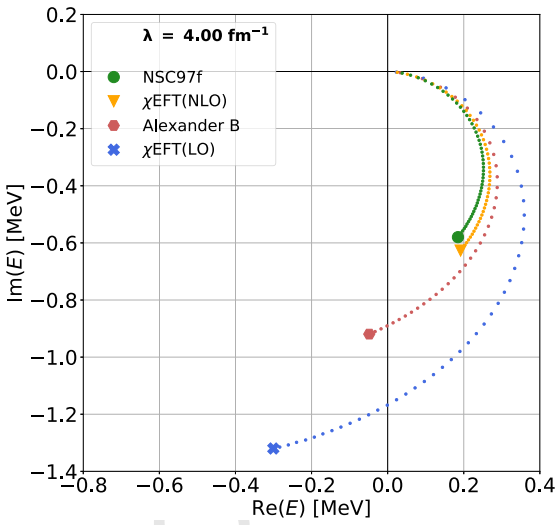

Fig. 2. Trajectories of the Λnn resonance pole in the complex energy plane determined by a decreasing attractive strength $d_\lambda^{I=1,S=1/2}$ for selected sets of ΛN scattering length, calculated at $\lambda=4.00$ fm^{-1}. Larger symbols stand for the physical position of the Λnn pole ($d_\lambda^{I=1,S=1/2}=0$).

As we have already pointed out, the possible existence of bound Λnn and ${}^3_\Lambda$H* states has been quite convincingly ruled out in several theoretical studies [4–10]. Our $\not\pi$EFT findings support their conclusions.

3.1. A Λnn resonance?

We start our study of three-body hypernuclear continuum states with the Λnn system. To understand the cutoff dependence of our theory we present, in Fig. 1, the trajectories $E_{\Lambda nn}(d_\lambda^{I=1,S=1/2},\lambda)$ of the Λnn resonance pole, calculated using the IACCC method for different values of cutoff λ, and for a representative set of $a_s^{\Lambda N}$ - NSC97f. With decreasing attraction of $V_3^{\rm IACCC}$, the resonance poles move along a circular trajectory in the complex energy plane starting from the $\Lambda+n+n$ threshold to the physical end point where $d_\lambda^{I=1,S=1/2}=0$. The figure suggests that the trajectories $E_{\Lambda nn}(d_\lambda^{I=1,S=1/2},\lambda)$ and the physical end points converge with increasing cutoff, and already at $\lambda=2.5$ fm^{-1} we approach stabilized results.

Repeating the same calculations for all sets of scattering lengths given in Table 1, we find that regardless the cutoff value, the imaginary part of the physical solution $\mathrm{Im}(E^\lambda_{\Lambda nn})$ lies in the interval $-1.32\le \mathrm{Im}(E^\lambda_{\Lambda nn})\le -0.58$ MeV for all $a_s^{\Lambda N}$ sets. In contrast, the real part $\mathrm{Re}(E^\lambda_{\Lambda nn})$ exhibit large cutoff dependence. As shown in Fig. 1 for the NSC97f case, the pole moves with increasing λ from the unphysical part of the Riemann sheet ($\mathrm{Re}(E)<0$, $\mathrm{Im}(E)<0$; third quadrant) towards the physical one ($\mathrm{Re}(E)>0$, $\mathrm{Im}(E)<0$; fourth quadrant).

In Fig. 2 we compare the trajectories $E_{\Lambda nn}(d_\lambda^{I=1,S=1/2},\lambda)$ for the different values of ΛN scattering lengths, Table 1, at cutoff $\lambda=4$ fm^{-1}. From the figure, we can deduce that the existence of a physically observable Λnn resonance is very sensitive to the ΛN interaction. The latter must be strong enough to ensure the pole's location in the fourth quadrant of a complex energy plane. The figure and Table 1 show that with increasing size of the spin-averaged scattering length $\bar a^{\Lambda N}=3/4a_1^{\Lambda N}+1/4a_0^{\Lambda N}$ the Λnn pole trajectories move closer to the $\Lambda+n+n$ threshold. Moreover, by increasing the cutoff λ the physical Λnn pole is shifted closer to or into the fourth quadrant. In this sense the pole position in the renormalization group invariant limit $\lambda\to\infty$ could be considered as the most favorable to the existence of an observable resonance. Nevertheless, in the $\lambda\to\infty$ limit only two sets of $a_s^{\Lambda N}$ - NSC97f and χEFT(NLO) undoubtedly predict a physical resonance. From the results shown in Fig. 2 we can roughly estimate that $\bar a^{\Lambda N}\approx 1.7$ fm^{-1} is the minimal value for the Λnn pole to enter the fourth quadrant, becoming a physical resonance. It should be noted that though the size of $\bar a^{\Lambda N}$ plays a dominant role, one should take into account also the effect of the three-body force which might introduce more complicated dependence on $a_0^{\Lambda N}$ and $a_1^{\Lambda N}$.

3.2. The hypertriton excited state ${}^3_\Lambda$H$^*(J^\pi=3/2^+)$

The excited state of the hypertriton ${}^3_\Lambda$H$^*(J^\pi=3/2^+)$ might be considered as a good candidate for a near-threshold resonance. Indeed, several works demonstrated an emergence of a bound state by increasing rather moderately the ΛN interaction strength. Applying the IACCC method we follow the pole trajectory given by the amplitude of auxiliary 3-body force $d_\lambda^{I=0,S=3/2}$ from a bound region to its physical position in a Λ+deuteron ($\Lambda+d$) continuum. In Fig. 3 we show the ${}^3_\Lambda$H* pole momentum $k=\sqrt{2\mu_{\Lambda d}[E({}^3_\Lambda\mathrm{H}^*)-E_B({}^2\mathrm{H})]}$, $\mu_{\Lambda d}=m_d m_\Lambda/(m_d+m_\Lambda)$, as a function of $d_\lambda^{I=0,S=3/2}$ for Alexander B ΛN scattering lengths and $\lambda=6$ fm^{-1}. We observe that with a decreasing auxiliary attraction the imaginary part of the momentum $\mathrm{Im}(k)$ decreases from positive value (bound state) to a negative value (unbound state) whereas the real part $\mathrm{Re}(k)$ remains equal to zero. This behavior is regarded as definition of a virtual state [50].

Repeating the calculations for various cutoffs and different ΛN scattering lengths, Table 1, we find ${}^3_\Lambda$H* to be a virtual state in all considered cases. As we have seen in the Λnn calculations, the energy of the virtual state E_v is stabilized at cutoffs $\lambda\gtrsim 4$ fm^{-1}.

The existence of the ${}^3_\Lambda$H* virtual state is further confirmed by the CSM. We do not see any sign of resonance for all sets of ΛN scattering lengths, cutoffs, or auxiliary 3-body force values $d_\lambda^{I=0,S=3/2}$. Odsuren et al. [51] have showed that the rotated discretized CSM continuum spectra reflect phenomena such as near-threshold virtual states, although one would naively assume that virtual states having $|\arg E|=\pi/2$ are beyond the reach of the CSM. From continuum level density they have extracted the scat-

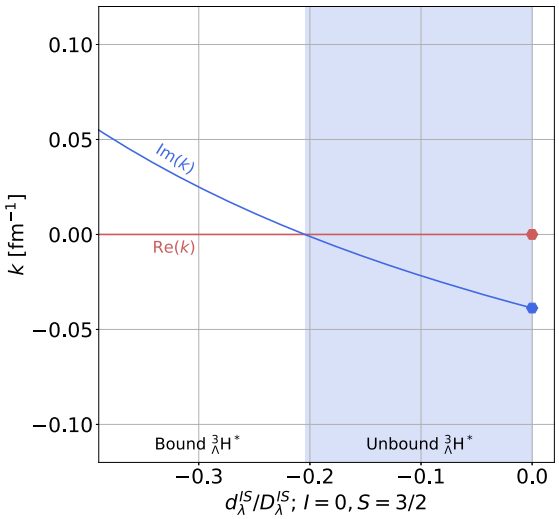

Fig. 3. Imaginary (blue) and real (red) parts of the ${}^3_\Lambda$H* pole momentum k as a function of $d_\lambda^{I=0,S=3/2}$, normalized to the physical three-body LEC $D_\lambda^{I=0,S=3/2}$. Unbound region is determined through the IACCC method. Dots mark the physical solution with for $d_\lambda^{I=0,S=3/2}=0$.

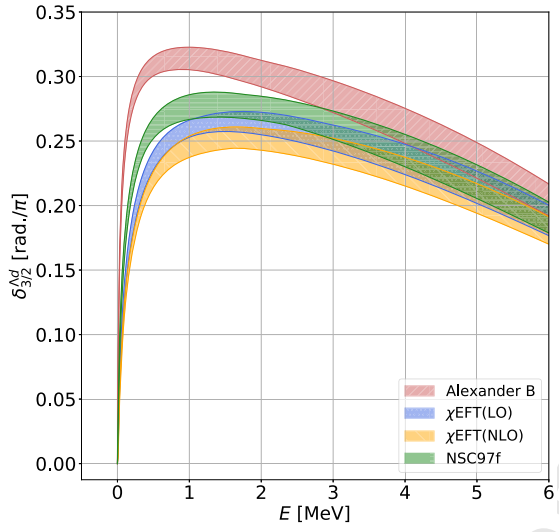

Fig. 4. S-wave Λd phase shifts in the $J^\pi=3/2^+$ channel $\delta^{\Lambda d}_{3/2}$ as a function of energy E above the $\Lambda+d$ threshold, extracted from the continuum level density of the rotated CSM spectra. The phase-shifts are calculated for cut-off $\lambda=6$ fm^{-1} and several ΛN interaction strengths. Shaded areas mark uncertainty introduced by the rotation angle θ within interval $15^\circ<\theta<20^\circ$.

tering phase shifts which revealed enhancement due to the vicinity of a the pole [51,52]. Following this approach we calculated the Λd s-wave phase shifts $\delta^{\Lambda d}_{3/2}$ for the $J^\pi=3/2^+$ channel. The calculated phase shifts, presented in Fig. 4, exhibit clear enhancement close to threshold implying proximity of a pole. The shaded areas in the figure reflect the phase shift dependence on rotation angle θ, which we checked for a rather broad interval $15^\circ<\theta<20^\circ$.

The scattering length $a^{\Lambda d}_{3/2}$ and effective range $r^{\Lambda d}_{3/2}$ extracted from the Λd phase shifts reveal through their sign, negative $a^{\Lambda d}_{3/2}$ and positive $r^{\Lambda d}_{3/2}$, the existence of a virtual state [53]. Using $a^{\Lambda d}_{3/2}, r^{\Lambda d}_{3/2}$ the virtual state binding momentum $k_v=\sqrt{2\mu_{\Lambda d}E_v}$ can be approximated by

$$k_v=\frac{i}{r^{\Lambda d}_{3/2}}\left(1-\sqrt{1-\frac{2\,r^{\Lambda d}_{3/2}}{a^{\Lambda d}_{3/2}}}\right). \tag{11}$$

Table 2
Calculated Λd scattering lengths $a^{\Lambda d}_{3/2}$, effective ranges $r^{\Lambda d}_{3/2}$, and virtual state energies E_v in $J^\pi=3/2^+$ channel for several ΛN interaction strengths and cutoff $\lambda=6$ fm^{-1}. Results of two different methods are presented - the continuum level density of rotated CSM spectra and the IACCC method. For the CSM we obtain E_v using relation (11), for the IACCC using the relation $a^{\Lambda d}_{3/2}=-i/\sqrt{2\mu_{\Lambda d}E_v}$. The scattering length and effective range are given in fm, E_v in MeV.

	CSM			IACCC	
	$a^{\Lambda d}_{3/2}$	$r^{\Lambda d}_{3/2}$	E_v	$a^{\Lambda d}_{3/2}$	E_v
Alexander B	-17.3	3.6	-0.08	-25.7	-0.042
NSC97f	-10.8	3.8	-0.18	-16.1	-0.108
χEFT(LO)	-8.5	3.5	-0.28	-12.8	-0.169
χEFT(NLO)	-7.6	3.6	-0.34	-11.7	-0.205

In Table 2 we present the IACCC results for E_v, and an estimate $a^{\Lambda d}_{3/2}=-i/\sqrt{2\mu_{\Lambda d}E_v}$ for the scattering length, together with the scattering parameters $a^{\Lambda d}_{3/2}$ and $r^{\Lambda d}_{3/2}$ extracted from the CSM calculations and the resulting estimate for E_v, Eq. (11). Inspecting the table, one might naively expect clear monotonic dependence of E_v on the spin-triplet scattering length $a_1^{\Lambda N}$. However, the dominance of $a_1^{\Lambda N}$ is undermined by the 3-body force in the $(I,S)=(0,3/2)$ channel, fixed by $B_\Lambda({}^4_\Lambda\text{H}^*)$. Comparing the IACCC and CSM results, one clearly see that both approaches are in mutual agreement, they exhibit the same dependence on the ΛN interaction strength, though, the CSM yields larger estimates for $|E_v|$. It is a well known drawback of the CSM that eigenvalues in a vicinity of the threshold start to be affected by inaccuracies caused by complex arithmetic.

Concluding this section, we see that at LO $\not\pi$EFT firmly predicts the excited state of hypertriton ${}^3_\Lambda\text{H}^*(J^\pi=3/2^+)$ to be a virtual state in the vicinity of the $\Lambda-d$ threshold. This result has important implications for prospective experimental search of this state. Experimental observation of ${}^3_\Lambda$H* as a resonance state seems to be highly unlikely. Instead, there is a near-threshold virtual state which should be seen through the enhancement of s-wave Λd phase shifts in the $J^\pi=3/2^+$ channel as demonstrated in Fig. 4.

4. Conclusions

In this work we have presented the first comprehensive $\not\pi$EFT study of continuum hypernuclear ΛNN trios. The underlying nucleon and hyperon interactions were described within a $\not\pi$EFT at LO, with the LECs fixed by 2-body low energy observables and experimental input from 3- and 4-body s-shell systems. The Λnn and ${}^3_\Lambda$H* energies were then obtained as predictions of the theory. In view of poor low energy ΛN scattering data we considered several sets of ΛN scattering lengths, whereas the NN interaction remained constrained by experiment [18].

Few-body wave functions were described within a correlated gaussians basis. Bound state solutions were obtained using the SVM. The continuum region was studied employing two independent methods - the IACCC method and CSM.

The $\not\pi$EFT predicts that both Λnn and ${}^3_\Lambda$H* are unbound. Tuning the 3-body LECs to put the Λnn or ${}^3_\Lambda$H* binding energy on threshold, yielded considerable discrepancy between the calculated and measured B_Λ in the $A=4,5$ hypernuclei. Our findings further strengthen the conclusions of previous theoretical studies that both states are unbound [4–10,16,17].

Our LO $\not\pi$EFT calculations predict Λnn and ${}^3_\Lambda$H* to be near-threshold continuum states. We thus anticipate that the EFT truncation error is small due to low characteristic momenta and thus higher order corrections would not change our results qualitatively. We conclude that position of the Λnn pole depends strongly on the spin independent scattering length $\bar{a}^{\Lambda N}$. For $\bar{a}^{\Lambda N}\geq 1.7$ fm^{-1} the Λnn pole becomes a physical resonance close to threshold

with $E_r \leq 0.3$ MeV, and a large width most likely in the range $1.16 \leq \Gamma \leq 2.00$ MeV. If observed, the position of the Λnn resonance can yield tight constraints on the ΛN scattering length. We note, however, that the exact position of the Λnn depends both on $a_0^{\Lambda N}$ and $a_1^{\Lambda N}$, and also on subleading $\not\pi$EFT terms neglected here. The excited state of hypertriton ${}^3_\Lambda\mathrm{H}^*$ was firmly predicted to be a near-threshold virtual state regardless of the value of $a_s^{\Lambda N}$. We have demonstrated that this virtual state has a strong effect on the Λd s-wave phase shifts in $J^\pi = 3/2^+$ channel.

Declaration of competing interest

The authors declare that they have no known competing financial interests or personal relationships that could have appeared to influence the work reported in this paper.

Acknowledgements

We are grateful to Avraham Gal for valuable discussions and careful reading of the manuscript. This work was partly supported by the Czech Science Foundation GACR grant 19-19640S. The work of NB was supported by the PAZY Foundation and by the Israel Science Foundation grant 1308/16.

Uncited references

[32] [33] [36] [37] [38] [39] [40] [41]

References

[1] A. Gal, E.V. Hungerford, D.J. Millener, Rev. Mod. Phys. 88 (2016) 035004.
[2] D.H. Davis, Nucl. Phys. A 754 (2005) 3c.
[3] C. Rappold, et al., HypHI Collaboration, Phys. Rev. C 88 (2013) 041001(R).
[4] B.W. Downs, R.H. Dalitz, Phys. Rev. 114 (1959) 593.
[5] H. Garcilazo, J. Phys. G 13 (1987) 63.
[6] A. Gal, H. Garcilazo, Phys. Lett. B 736 (2014) 93.
[7] H. Garcilazo, T. Fernández-Caramés, A. Valcarce, Phys. Rev. C 75 (2007) 034002; H. Garcilazo, T. Fernández-Caramés, A. Valcarce, Phys. Rev. C 76 (2007) 034001.
[8] H. Garcilazo, A. Valcarce, Phys. Rev. C 89 (2014) 057001.
[9] K. Miyagawa, H. Kamada, W. Glöckle, V. Stoks, Phys. Rev. C 51 (1995) 2905.
[10] E. Hiyama, S. Ohnishi, B.F. Gibson, Th.A. Rijken, Phys. Rev. C 89 (2014) 061302(R).
[11] S.-I. Ando, U. Raha, Y. Oh, Phys. Rev. C 92 (2015) 024325.
[12] F. Hildenbrand, H.-W. Hammer, Phys. Rev. C 100 (2019) 034002.
[13] S. Bleser, M. Bölting, T. Gaitanos, J. Pochodzalla, F. Schupp, M. Steinen, AIP Conf. Proc. 2130 (2019) 030001.
[14] JLab, E12-17-003, https://misportal.jlab.org/mis/physics/experiments/viewProposal.cfm?paperId=917, 2020.
[15] JLab proposal P12-19-002, https://www.jlab.org/exp_prog/proposals/19/PR12-19-002.pdf, 2020.
[16] V.B. Belyaev, S.A. Rakityansky, W. Sandhas, Nucl. Phys. A 803 (2008) 210.
[17] I.R. Afnan, B.F. Gibson, Phys. Rev. C 92 (2015) 054608.
[18] L. Contessi, N. Barnea, A. Gal, Phys. Rev. Lett. 121 (2018) 102502.
[19] U. van Kolck, Nucl. Phys. A 645 (1999) 273.
[20] P.F. Bedaque, H.-W. Hammer, U. van Kolck, Nucl. Phys. A 676 (2000) 357.
[21] N. Barnea, L. Contessi, D. Gazit, F. Pederiva, U. van Kolck, Phys. Rev. Lett. 114 (2015) 052501.
[22] J. Kirscher, N. Barnea, D. Gazit, F. Pederiva, U. van Kolck, Phys. Rev. C 92 (2015) 054002.
[23] L. Contessi, A. Lovato, F. Pederiva, A. Roggero, J. Kirscher, U. van Kolck, Phys. Lett. B 772 (2017) 839.
[24] J. Kirscher, E. Pazy, J. Drachman, N. Barnea, Phys. Rev. C 96 (2017) 024001.
[25] K. Varga, Y. Suzuki, Phys. Rev. C 52 (1995) 2885.
[26] Y. Suzuki, K. Varga, Stochastic Variational Approach to Quantum-Mechanical Few-Body Problems, Springer, 1998.
[27] B. Bazak, M. Eliyahu, U. van Kolck, Phys. Rev. A 94 (2016) 052502.
[28] G. Alexander, U. Karshon, A. Shapira, et al., Phys. Rev. 173 (1968) 1452.
[29] Th.A. Rijken, V.G.J. Stoks, Y. Yamamoto, Phys. Rev. C 59 (1999) 21.
[30] H. Polinder, J. Haidenbauer, U.-G. Meißner, Nucl. Phys. A 779 (2006) 244.
[31] J. Haidenbauer, S. Petschauer, N. Kaiser, U.-G. Meißner, A. Nogga, W. Weise, Nucl. Phys. A 915 (2013) 24.
[32] G.A. Miller, M.K. Nefkens, I. Slaus, Phys. Rep. 1 (1990) 194.
[33] C. Van Der Leun, C. Alderliesten, Nucl. Phys. A 380 (1982) 261.
[34] J. Augilar, J.M. Combes, Commun. Math. Phys. 22 (1971) 269; E. Balslev, J.M. Combes, Commun. Math. Phys. 22 (1971) 280.
[35] S. Aoyama, T. Myo, K. Katō, K. Ikeda, Prog. Theor. Phys. 116 (2006) 1.
[36] N. Moiseyev, Non-Hermitian Quantum Mechanics, Cambridge University Press, 2011.
[37] J.Zs. Mezei, A.T. Kruppa, K. Varga, Few-Body Syst. 41 (2007) 233.
[38] N. Moiseyev, P.R. Certain, F. Weinhold, Mol. Phys. 36 (1978) 1613.
[39] R. Yaris, P. Winkler, J. Phys. B 11 (1978) 1475.
[40] W. Horiuchi, Y. Suzuki, Few-Body Syst. 54 (2013) 2407.
[41] J. Usukura, Y. Suzuki, Phys. Rev. A 66 (2002) 010502(R).
[42] T.D. Fedorov, et al., Few-Body Syst. 45 (2009) 191.
[43] V.M. Kukulin, V.M. Krasnopol'sky, J. Phys. A 10 (1977) 33; V.M. Krasnopol'sky, V.I. Kukulin, Phys. Lett. A 69 (1978) 251; V.I. Kukulin, V.M. Krasnopol'sky, M. Miselkhi, Sov. J. Nucl. Phys. 29 (1979) 421.
[44] N. Tanaka, Y. Suzuki, K. Varga, R.G. Lovas, Phys. Rev. C 59 (1999) 1391.
[45] R. Lazauskas, E. Hiyama, J. Carbonell, Phys. Lett. B 791 (2019) 335, and references therein.
[46] N. Tanaka, Y. Suzuki, K. Varga, Phys. Rev. C 56 (1997) 562.
[47] V.I. Kukulin, V.M. Krasnopol'sky, J. Horáček, Theory of Resonances, Principles and Applications, Kluwer Academic Publishers, 1989.
[48] J. Horáček, L. Pichl, Commun. Comput. Phys. 21 (2017) 1154.
[49] L. Contessi, N. Barnea, A. Gal, AIP Conf. Proc. 2130 (2019) 040012.
[50] J.R. Taylor, Scattering Theory: Quantum Theory on Nonrelativistic Collisions, 99 edition, Willey, 1972.
[51] M. Odsuren, Y. Kikuchi, T. Myo, G. Khuukhenkhuu, H. Masui, K. Katō, Phys. Rev. C 95 (2017) 064305.
[52] M. Odsuren, K. Katō, M. Aikawa, T. Myo, Phys. Rev. C 89 (2014) 034322.
[53] T. Hyodo, Phys. Rev. Lett. 111 (2013) 132002.